



REPORT NO. 79

APRIL, 1954.

THE COLLEGE OF AERONAUTICS

CRANFIELD

An Experimental Investigation of the Pressure
Distributions on Five Bodies of Revolution
at Mach Numbers of 2.45 and 3.19.



-by-

G.B. Marson, B.Sc.,

*R.E. Keates, B.Sc., D.C.Ae.,

*W. Socha, D.C.Ae.

of The Department of Aerodynamics.

S U M M A R Y

Measurements have been made in the College of Aeronautics $2\frac{1}{2}$ " x $2\frac{1}{2}$ " intermittent high speed tunnel of the pressure distributions on five non lifting bodies of revolution of different nose angles at zero incidence. The tests were made at Mach numbers of 2.45 and 3.19.

The results are compared with the pressure distributions given by two approximate theoretical methods, and good agreement is found at the Mach numbers used.

*These authors submitted part of this work as a part requirement for the award of the Diploma of the College of Aeronautics.

<u>§1.</u>	<u>List of Contents</u>	<u>Page</u>
2.	List of Symbols	3
3.	Introduction	4
4.	Description of the theoretical methods	4
5.	Experimental apparatus and method	7
6.	Results	8
7.	Conclusions	9
8.	Acknowledgements	10
9.	References	10
<u>Appendix</u>		
	Example of the application of the modified ogive of curvature method to Ogive III at M = 2.45.	11
<u>Tables</u>		
1.	Geometry of the bodies	13
2.	Summary of results	13
<u>Figures</u>		
1.	General view of the wind tunnel	
2.	Working section of the wind tunnel	
3.	Block diagram of the tunnel circuit	
4.	Sting, showing pressure connections to the model	
5.	Ogives I, II, and III	
6.	Pressure distribution on Cone at M = 2.45	
7.	" " " " " M = 3.19	
8.	" " " Ogive I at M = 1.8	
9.	" " " " I " M = 2.45	
10.	" " " " II " M = 1.8	
11.	" " " " II " M = 2.45	
12.	" " " " III " M = 1.8	
13.	" " " " III " M = 2.45	
14.	" " " " III " M = 3.19	
15.	" " " " IV " M = 2.45	
16.	" " " " IV " M = 3.19	
17.	" " " " V " M = 2.45	
18.	" " " " V " M = 3.19	

§2. List of Symbols

A-S	(Suffix) referring to axi-symmetric flow
C_p	pressure coefficient = $\frac{p - p_o}{\frac{\rho}{2} p_o M_o^2}$
M	Mach number
p	surface static pressure
p_N	surface static pressure at nose
p_P	surface static pressure at an arbitrary point P
$p_{stag.}$	surface stagnation pressure
Δp	pressure difference
u_o	free stream velocity
x	streamwise co-ordinate, expressed as a fraction of body length
y	crosswind co-ordinate, expressed as a fraction of body length
l/d	fineness ratio = $\frac{\text{length of body}}{\text{max. diameter of body}}$
θ	angle between body axis and tangent to body profile
θ_s	nose semi-angle of body
χ	nose semi-angle of equivalent ogive of curvature
ν	Prandtl Meyer angle
α	ratio of specific heats
ρ_o	free stream density
2-D	(Suffix) referring to two dimensional flow
o	(Suffix) referring to free stream conditions.

§3. ...

§3. Introduction

Some rapid approximate methods or variants of methods of calculating the pressure distributions on non-lifting ogival heads at supersonic speeds have been described in a recent paper by Bolton-Shaw and Zienkiewicz.¹

These methods allowed a considerable saving in computing time as compared with the more accurate method of characteristics or Van Dyke's second order theory, whilst in particular cases for which a comparison was made they appeared to give good agreement with these more accurate methods. These approximate methods varied however in their range of applicability and in rapidity and from this point of view two in particular seemed more promising than the others.

The purpose of the present work was to extend the comparison by obtaining experimental pressure distributions for bodies with a wide range of nose angles and for a wide range of Mach numbers and to use these pressure distributions as a further guide to the reliability of the more promising approximate methods.

Details of the geometry of the five bodies are given in Table I. Ogives, III, IV and V belong to a particular family of curved head shapes.

Ogives I, II, and III were originally tested in the N.P.L. 9" x 3" high speed wind tunnel at a Mach number of 1.8 as described in Ref. 7. The present paper describes further tests made at The College of Aeronautics on these three ogives, together with tests of ogives IV and V, at $M = 2.45$. Ogives III, IV and V were also tested at $M = 3.19$.

§4. Description of the approximate theoretical methods

For convenience a brief summary of the methods developed by Bolton Shaw and Zienkiewicz is given below.

(i) The λ -method for a circular arc ogive

It has been shown by Zienkiewicz² that for a circular arc ogive in a supersonic stream, the decrease in pressure from the nose to any point P on the ogive surface, is proportional to the decrease in pressure from the leading edge of a two-dimensional aerofoil section, having the same profile as the ogive, to a corresponding point P on the aerofoil, provided that the Mach number and pressure just downstream of the nose and leading edge are the same.

/Thus ...

Thus

$$(p_N - p_P)_{A-S} = \lambda (p_N - p_P)_{2-D} \dots\dots\dots(1)$$

where λ depends only on the free stream Mach number M_o and the nose angle θ_s .*

In equation (1), p_N is the constant pressure at the nose of both the axi-symmetric and two-dimensional profiles.

It should be noted that in this method, the surface stagnation pressure is constant, and is the same on both body and aerofoil, but the free stream Mach number ahead of the aerofoil will not equal M_o .

(ii) The λ step-by-step method for an arbitrary head shape

For this method it is assumed that the expansion of the flow between any point P on the surface and an adjacent point Q, is the same as would have been obtained by the expansion of the flow around the equivalent circular arc ogive passing through P and Q. It follows from equation (1) that

$$(p_Q - p_P)_{A-S} = \lambda (p_Q - p_P)_{2-D} \dots\dots\dots(2)$$

The value of λ depends on the nose angle, χ , of the equivalent ogive of curvature, and an equivalent free stream Mach number, M_E . The value of M_E has first to be found by trial and error such that the pressure at P agrees with that obtained in the previous step. After the value of M_E is found, the value of λ can be obtained from the charts in Ref. 1. The pressure at the adjacent point Q then follows from an application of equation (2).

(iii) The ogive of curvature method

It was found from applications of the λ step-by-step method that the ratio of the static to stagnation pressure at a point P on an arbitrary head shape at a free stream Mach number M_o was practically the same as at P on the equivalent ogive of curvature at P at the same value of M_o (i.e. in (ii) above, $M_E = M_o$). Since the pressures on the ogive of curvature can be calculated from equation (1), the pressure on any arbitrary head shape can be quickly obtained. The only information required is the distribution of the surface inclination to the axis, θ , and the nose angle χ of the equivalent local ogive
/of curvature. ...

* Values of λ are given in graphical form in Ref. 1, but an extended and modified set of values for λ has been evaluated by Zienkiewicz.⁸

of curvature. The stagnation pressure on the local ogive of curvature was taken as equal to that at the nose of the actual body but for the bodies examined the change in stagnation pressure across the nose shock was very small, and the method could equally well have been developed on the assumption that the stagnation pressures ahead of the nose shock for the body and the equivalent ogive of curvature were the same.

(iv) The log p- θ method

It was found that for convex ogival head shapes, $\log \frac{p_P}{p_N}$ was proportional to $(\theta_s - \theta)$, provided that $2M_0 \tan \frac{\chi}{2} > 0.4$, where θ_s is the nose semi-angle of the body and χ is the nose semi-angle of the equivalent ogive of curvature. This method gives good results for bodies of small nose angle, and the results of this method are here compared with the experimental pressure distributions obtained for Ogives I, II and III. (See Figs.8-13).

(v) The modified ogive of curvature method

It was found that for head shapes having large nose angles, both methods (iii) and (iv) gave consistently low values of pressure on the downstream end of the head. It was then suggested by Zienkiewicz that better agreement could be obtained if the condition for the same stagnation pressure aft of the nose shock on the local ogive of curvature as at the nose of the actual body be replaced by the condition of the same stagnation pressure ahead of the nose shocks since as noted above the original data examined did not allow one to decide which of these conditions was likely to lead to more accurate results.

In this modified method the values of χ are calculated from the $\theta - x$ distribution at a selected number of values of x . At each station a value of $\lambda(M_0, \chi)$ is selected for the given free stream Mach number M_0 , and from equation (1), the values of p_P and $C_p = \frac{p_P - p_0}{\frac{1}{2} \rho_0 u_0^2}$ can be obtained once p_N is determined.

The value of p_N , the pressure at the nose of the equivalent ogive of curvature, is obtained from cone tables⁴ for the given values of χ , M_0 and α and the same free stream stagnation pressure as that ahead of the body. The stagnation pressure on the equivalent ogive of curvature is therefore taken to be the stagnation pressure on the surface of the cone of nose semi-angles χ . For small values of χ , however, the loss of stagnation pressure across the nose shock wave is very small, and as already remarked the stagnation pressure on the surface of the cone could then equally well be taken as the same as the

/freestream ...

freestream stagnation pressure. Large values of χ can occur near the nose of bodies of large nose-angle but even then the value of χ drops rapidly further downstream.

A pro forma suitable for this method is given in the Appendix. It will be evident from what follows that this method offers the best combination of speed and accuracy for computing the surface pressure distribution for a wide variety of head shapes and Mach numbers.

§5. Experimental apparatus and Method

The tests were conducted in the $2\frac{1}{2}$ " x $2\frac{1}{2}$ " intermittent supersonic wind tunnel. A general view of part of the tunnel with the working section open is shown in Fig. 1. The working section with a model fitted in position is shown in Fig. 2. Fig. 3 shows a block diagram of the tunnel circuit. In normal operation, the pump draws air from the vacuum chamber, and exhausts into the dry air bag. When the tunnel is running, air flows from the dry air bag through the silica gel bed and working section into the vacuum tanks. The normal available running time with one vacuum tank is about 45 secs. at a Mach number of 2.45. The change in pressure in the vacuum tank during the run is from about 100 mm.Hg. absolute to 300 mm. Hg. absolute.

The ogival heads, Fig. 4, were supported at zero incidence on a sting. The interior of each model was divided into two compartments; pressure tapings being taken from each to a manometer via hypodermic tubing and a pneumatic clamp. Fig. 5 shows details of the sting and the method of attaching the models to the hypodermic tubing. Pressure holes (0.025in. diameter) were drilled normal to the surface to connect the inner compartments with the surface. Each compartment contained five or six tapings, of which all but one were sealed in any one test. In order to check the axial pressure distribution and the symmetry of the flow in the working section, a conical head of similar length and fineness ratio to ogive III was placed in the tunnel. Preliminary measurements demonstrated the need for the pressure readings to be obtained with the greatest possible accuracy and the normal vertical multi-tube manometer was found unsuitable. A manometer was therefore constructed using three 0.25in. inside diameter tubes close together. These were connected to the two pressure tapings on the body, and a working section tapping on the flat top liner of the tunnel (p_0). The values of $p-p_0$ were then read off directly on a height gauge. An accuracy of about 0.003ins. Hg. could be obtained by this method. The difference between

atmospheric and stagnation pressure was measured on a Chattock gauge, atmospheric pressure being measured on a Fortin barometer. Nevertheless, a variation of about 10% in $(p-p_0)$ was still observed at each tapping as the model was rotated through four angular positions. This variation showed no constant tendency for different tappings, and was therefore assumed to be due not to misalignment of the model in the stream, but rather to small imperfections in the flow, the body shape, or the pressure holes themselves.

The same procedure was adopted for the pressure plotting of the ogives. It was found that the experimental scatter, on rotation of the body, was rather less than in the case of the cone. In the previous tests made at the N.P.L. (Ref. 7) the mean value of the pressure at each hole was obtained from the four readings at 0° , 90° , 180° and 270° roll respectively. A correction to this mean pressure was then applied based on the non-uniformity of the surface pressure as measured on the cone at the same station in the tunnel, it being assumed that the non-uniformity was due to imperfections in the flow. In the results reported here of the College of Aeronautics measurements, no such corrections have been made.

§6. Results

From the manometer and Chattock gauge readings, a series of values of $\frac{p-p_0}{p_{stag_0}}$ was obtained along and around the cone. A theoretical curve of $\frac{p-p_0}{p_{stag_0}}$ vs M_0 for this cone was obtained from Kopal's tables.⁴ The mean value of M_0 was then read off corresponding to the mean value of $\frac{p-p_0}{p_{stag_0}}$ on the cone. This value agreed within 4% with that obtained from readings of the working section pressure divided by the free stream stagnation pressure.

In the case of the cone, a variation of about $\pm 7\%$ in $p-p_0$ was found along the body in the streamwise direction (see Figs. 6 and 7). Since the corresponding variation in Mach number was less than $\pm 3\%$, it was felt that to find a mean value of Mach number in the way described above was sufficiently accurate for the present purpose.

The values of the pressure coefficients were obtained from

$$C_p = \frac{p-p_o}{\frac{1}{2}\rho_o u_o^2} = \frac{p-p_o}{0.7 M_o^2 p_o} = \frac{(p-p_o)\left(1 + \frac{M_o^2}{5}\right)^{3.5}}{0.7 M_o^2 p_{stag_o}}$$

with α taken as equal to 1.4.

Figs. 6-18 show the pressure distributions obtained experimentally for the cone and the ogives, and the corresponding curves calculated by the modified ogive of curvature method are shown in Figs. 8-18.

In the case of Ogives I, II and III, a curve given by the log p- θ method is also shown (Figs. 8-13). The comparison of the experimental results and theoretical curves is summarised in Table II.

In general, both methods, when applicable, give results which coincide with experiment within the limits of the experimental error. The log p- θ method is comparable in accuracy with the ogive of curvature method in predicting the pressure distribution over the forward portion of Ogives I and II, but is less accurate over the rear of Ogive II. The latter body has the larger change in curvature. This log p- θ method is evidently unsuitable for Ogives such as III, whose change in curvature, especially near the nose, is large.

The modified ogive of curvature method predicts the pressure distribution with acceptable accuracy for Ogives III, IV and V, for which the changes in curvature are large. However, the method tends to under-estimate the values of C_p near the nose at $M = 2.45$ and to over-estimate them at $M = 3.19$ for Ogive V (nose angle 30°). Whether this is due to errors in the experimental results or an indication of the errors in the method when applied to bodies having larger nose angles than 30° must be left for future investigation. The theory does not predict the small recompression at the rear of the bodies shown by the experimental points. It is probable that this may be due to boundary layer effects on the body and possibly to effects due to the tunnel boundary layer.

§7. Conclusions

The experimentally obtained pressure distributions on five head shapes with nose angles up to 30° , at Mach numbers of 2.45 and 3.19, are given. They are compared with the rapid approximate methods of calculation due to Bolton-Shaw and Zienkiewicz.

It is shown that the modified ogive of curvature method

/can be ...

can be successfully used for the rapid prediction of pressure distributions on arbitrary convex head shapes, with nose angles up to at least 30° and for Mach numbers up to 3.2, to an accuracy better than $\pm 4\%$ of the nose value.

The log p- θ method provides a rapid method suitable for ogives whose nose angles are less than 15° , but it is less accurate than the modified ogive of curvature method over the rear portion of the ogives tested.

§8. Acknowledgements

The authors would like to thank Mr. G.M. Lilley, who supervised the work, and Mr. H.K. Zienkiewicz, for their valuable advice and encouragement, Mr. S.H. Lilley for preparing the apparatus, and the English Electric Company for the models.

REFERENCES

<u>No.</u>	<u>Authors</u>	<u>Title, etc.</u>
1.	B.W. Bolton-Shaw and H.K. Zienkiewicz	The Rapid, Accurate, Prediction of Pressure on Non-Lifting, Ogival Heads of Arbitrary Shape at Supersonic Speeds. English Electric Rep. No. L.A.t.034. (June 1952)
2.	H.K. Zienkiewicz	A Method for Calculating Pressure Distributions on Circular Arc Ogives at Zero Incidence at Supersonic Speeds, using the Prandtl Meyer flow relations. English Electric Rep. No. L.A.t.024, also A.R.C. 14,790; F.M. 1702. (1952).
3.	Ehret, Dorris, Rossow and Stevens	An Analysis of the applicability of the Hypersonic Similarity Law to the Study of Flow about Bodies of Revolution at Zero Incidence. N.A.C.A. T.N. 2250.
4.	Z. Kopal.	Supersonic Flow of air around Cones. Massachusetts Institute of Technology. Center of Analysis, Tech. Rep. No. 1. (1947).
5.	A. Ferri	Elements of the Aerodynamics of Supersonic Flows. MacMillan, New York, (1949).
6.	C.L. Dailey and F.C. Wood	Computation Curves for Compressible Fluid Problems. John Wiley & Sons, Inc. New York (1949).
7.	H.K. Zienkiewicz, A. Chinneck, C.J. Berry, and P.J. Peggs.	Experiments at $M = 1.8$ on Bodies of Revolution having Ogival Heads. A.R.C. 15,586; F.M. 1854 (1953).
8.	H.K. Zienkiewicz	Further Development of some Approximate Methods for Predicting Pressure Distribution on Non-Lifting Ogival Heads at Supersonic Speeds. To be published as an English Electric L.A.t. Report.

APPENDIX

Example of the application of the modified ogive of curvature method to Ogive III at M = 2.45.

The pressure is required at points on the profile given by $x = 0.08, 0.16, 0.24, 0.40, 0.56$. The values of θ and χ at these points can be obtained from

$$y = 0.0620 x + 0.0372 \log_{10} \left(1 + \frac{x}{0.125} \right)$$

$$\theta = \tan^{-1} y_1 \quad \text{where } y_1 = \frac{dy}{dx}, \quad y_2 = \frac{d^2y}{dx^2}$$

$$\chi = \cos^{-1} \left[\frac{1 + y_1^2 + y y_2}{(1 + y_1^2)^{3/2}} \right]$$

After finding p/p_{stag} at the nose of the equivalent ogive of curvature, the decrease in p/p_{stag} from this value to its value at the point concerned is determined as a fraction, λ , of the two dimensional decrease in p/p_{stag} over an aerofoil of the same profile.

For nose angles below about 10° , p_{stag} is almost equal to p_{stag_0} , and so for simplicity, steps (6) and (7) below might be omitted, giving (8) = $\frac{(4)}{(5)}$. However, to keep the procedure consistent, it is necessary to work in terms of p_{stag} , rather than p_{stag_0} , and so these two steps have been retained in the present argument.

Ogive III

$M_o = 2.45$

1	x	.08	.16	.24	.40	.56
2	χ	12.53	9.43	8.10	6.50	5.70
3	C_p at (2) for given M_o (i.e. nose C_p for local ogive of curvature)	.138	.086	.068	.047	.039
4	$p_N/p_o = 1 + 0.7 M_o^2 C_p$. (p_N = pressure at nose of local ogive of curve)	1.580	1.361	1.286	1.197	1.163
5	p_{stag_o}/p_o at given M_o (constant)	15.80	15.80	15.80	15.80	15.80
6	p_{stag}/p_{stag_o} at given M_o and χ . (Bow shock loss for equivalent ogive of curvature). Ref.6, Fig.3.2.	.997	.999	1.000	1.000	1.000
7	(5)x(6) = p_{stag}/p_o for equivalent ogive of curvature	15.75	15.78	15.80	15.80	15.80
8	(4)/(7) = p_N/p_{stag} = $\frac{\text{nose pres. on equiv. ogive}}{\text{stag. pres. for that point}}$	0.1003	.0864	.0814	.0757	.0737
9	ν_A at (8) = wave angle at nose of equivalent ogive. (Ref. 5).	30.70	33.05	34.01	35.12	35.63
10	$\chi - \theta$	2.00	1.53	1.40	0.95	0.65
11	(9)+(10)	32.70	34.58	35.40	36.07	36.28
12	p/p_{stag} at (11) (at P for two dimensional aerofoil) Ref. 5.	.0880	.0783	.0746	.0715	.0705
13	(8)-(12) = $(\Delta p/p_{stag})_{2-D}$.0117	.0078	.0068	.0042	.0032
14	λ at (2) for given M_o . Ref. 1, Fig.1, and Ref. 8.	.802	.772	.755	.696	.645
15	(13)x(14) = $(\Delta p/p_{stag})_{A-S}$.0094	.0060	.0051	.0029	.0021
16	(8)-(15) = $p/p_{stag_{A-S}}$.0903	.0801	.0763	.0728	.0716
17	(16)x(7) - 1 = $p/p_o - 1$.	.426	.265	.205	.150	.131
(18)	(17)/ $0.7 M_o^2 = C_p$.101	.063	.049	.036	.031

/Table I ...

TABLE I
Geometry of The Bodies

Ogive	Nose Semi-angle	Fineness Ratio	Equation of Profile
I	15.95°	3.5	$y = \frac{1}{7} [1 - (x - 1)^2]$
II	14.9°	3.5	$y = .09445x_1^5 - .2817x_1^4 - .3780x_1^3 - .2335x_1^2 - .01252x_1 + .19815 [1 - (1 - x_1)^{3/2}]$ where $x_1 = 0.9x$.
III	21°	4.5	$y = .0620x + .0372 \log_{10} \left(1 + \frac{x}{.05}\right)$.
IV	24°	4.5	$y = .0636x + .03286 \log_{10} \left(1 + \frac{x}{.0374}\right)$.
V	30°	4.5	$y = .0655x + .02782 \log_{10} \left(1 + \frac{x}{.0236}\right)$.

TABLE II

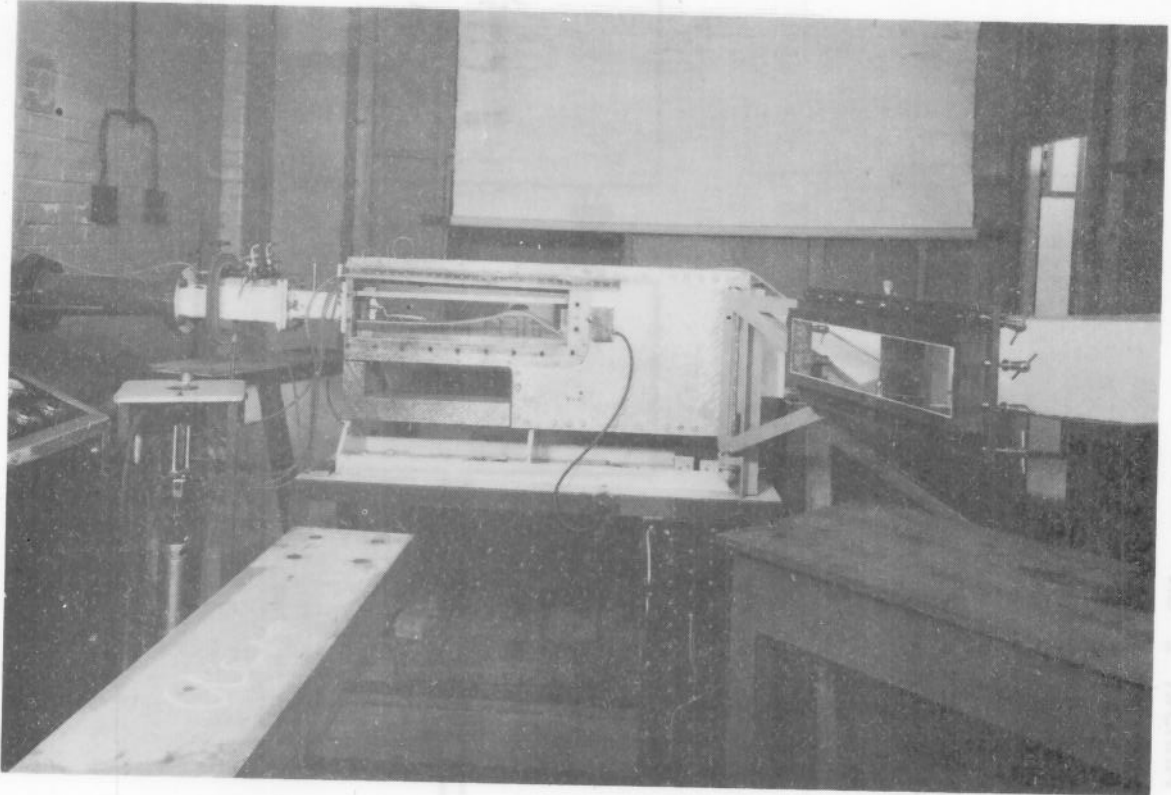
Summary of Comparison of Experimental Results with results given by the modified ogive of curvature method and the log p- method.

Ogive	M = 1.8	M = 2.45
I	Good agreement with both methods up to $x = 0.7$. O. of C.* method more accurate at rear, but overestimates C_p generally.	Good agreement with both methods up to $x = 0.7$. Log p- method considerably underestimates C_p at rear, whilst O. of C. method gives better agreement
II	Both methods underestimate C_p slightly up to $x = 0.6$. After this, the log p- method still underestimates C_p , but O. of C. method gives good agreement.	
III	O. of C. method gives reasonable agreement, but overestimates C_p at rear, and underestimates C_p at nose. Log p- method apparently breaks down beyond $x = 0.2$.	Reasonable agreement, with slight overestimation of C_p near nose and centre of ogive. Log p- method not suitable.

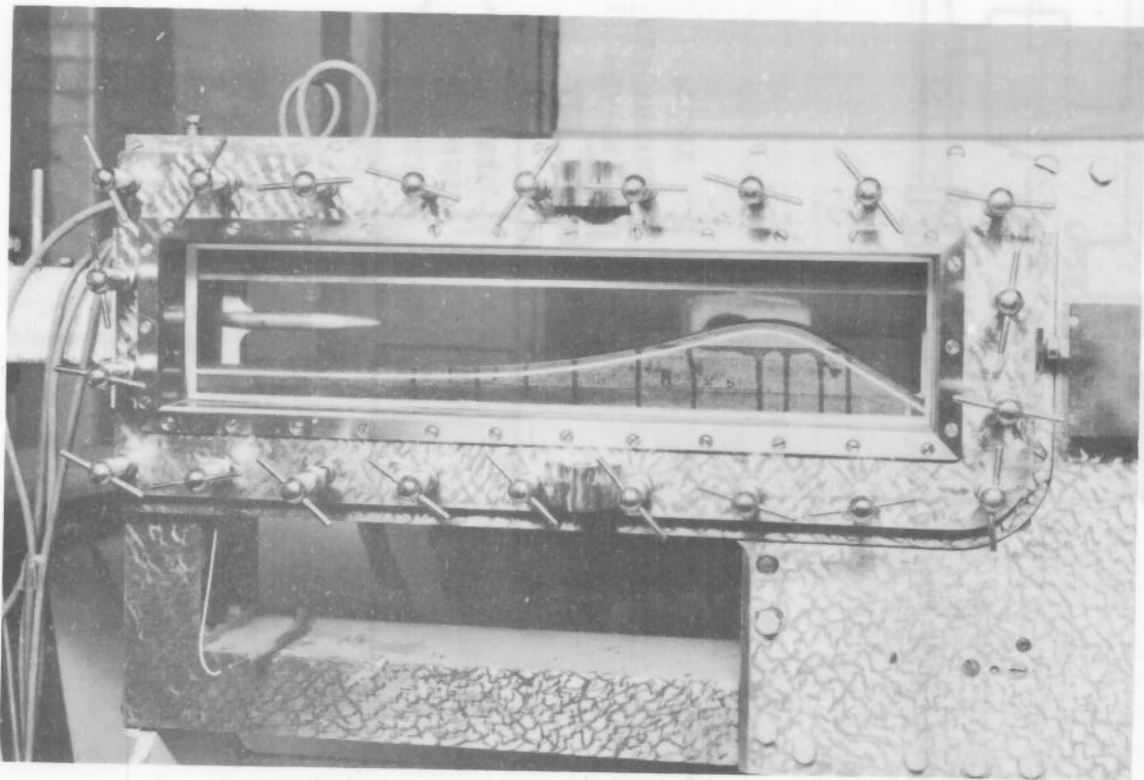
The following remarks refer to the O. of C. method; the log p- method was considered unsuitable for the cases covered.

Ogive	M = 2.45	M = 3.19
III	see above	Good agreement except that slight recompression at the rear end is not predicted.
IV	Slight underestimation of C_p near nose.	As for Ogive III.
V	Good agreement over most of body, with slight underestimation of C_p	Good agreement except for slight overestimation of C_p near nose.

* O. of C. method denotes the modified ogive of curvature method.



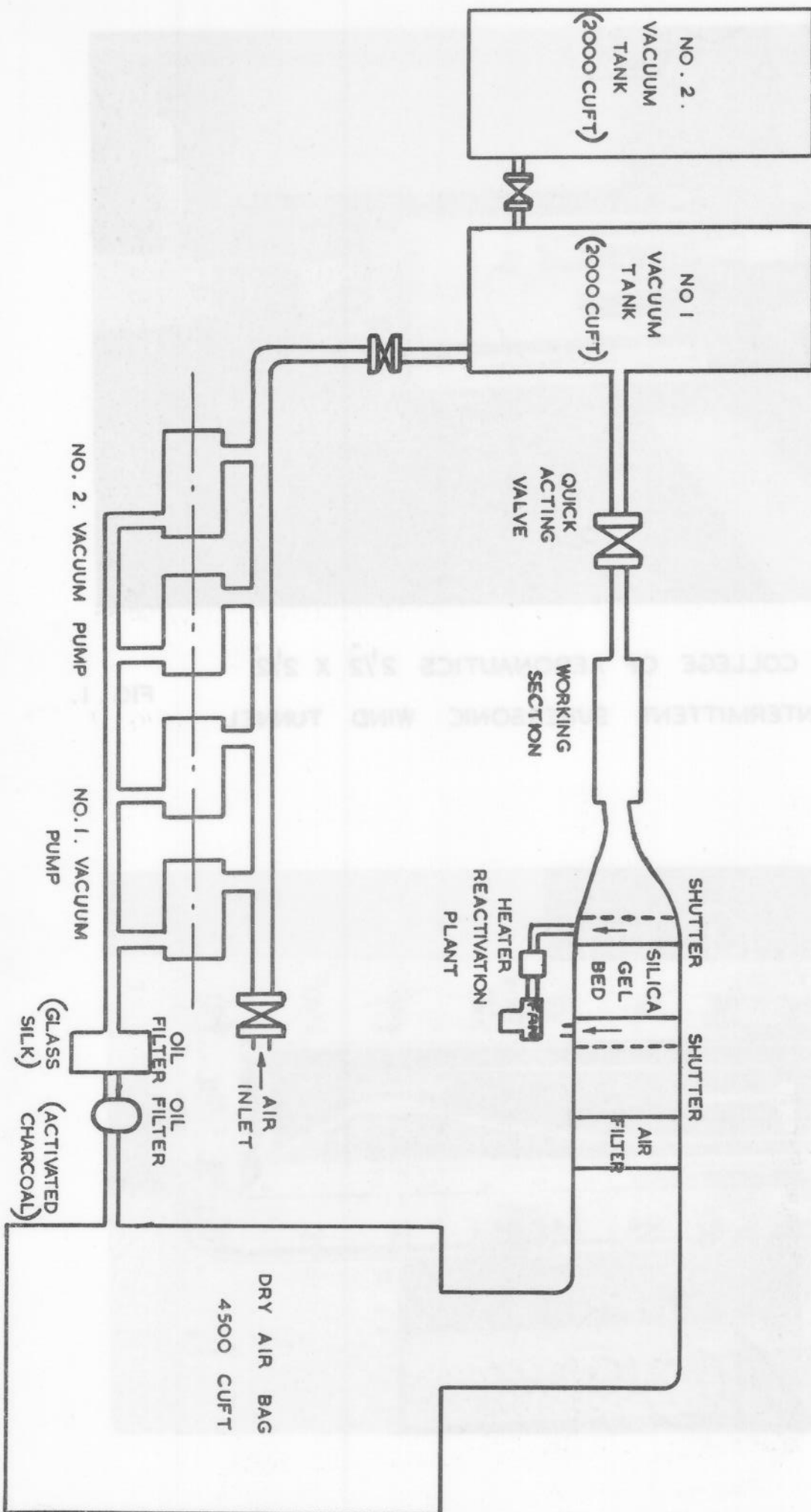
COLLEGE OF AERONAUTICS $2\frac{1}{2}$ " x $2\frac{1}{2}$ "
INTERMITTENT SUPERSONIC WIND TUNNEL FIG. 1.



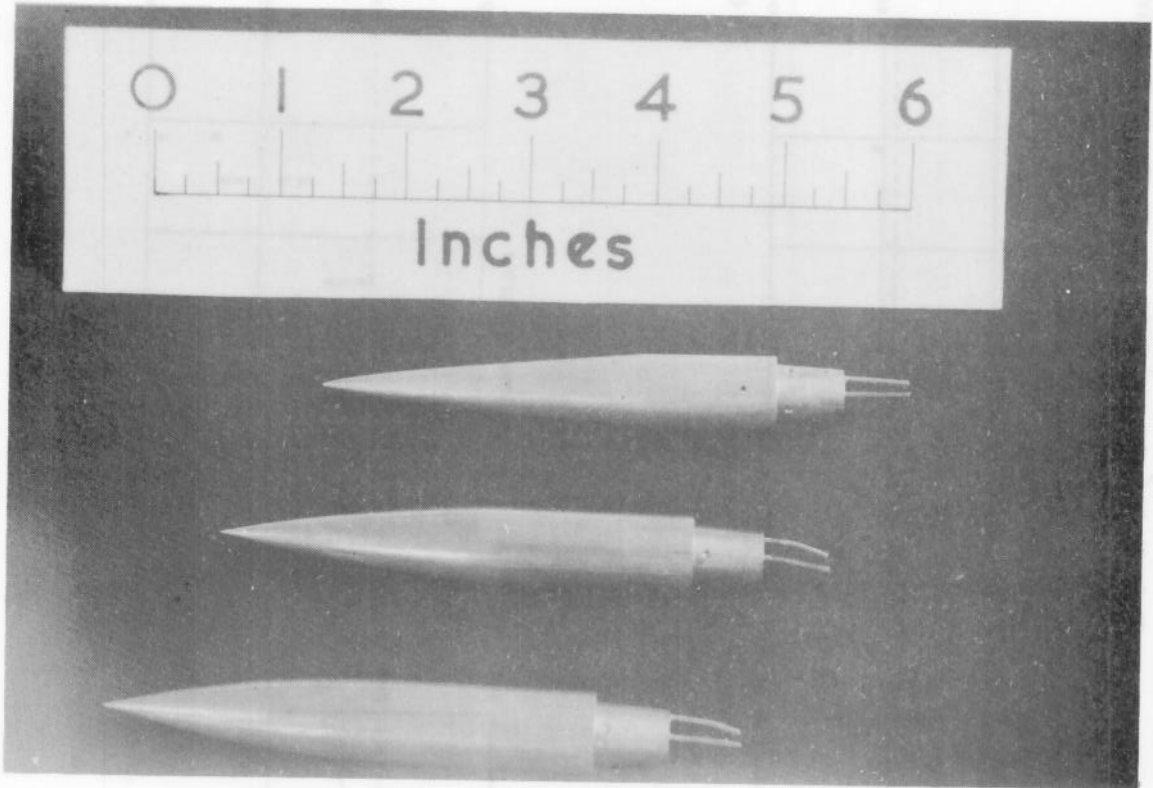
WORKING SECTION OF THE INTERMITTENT WIND TUNNEL.

FIG. 2

FIG. 3.

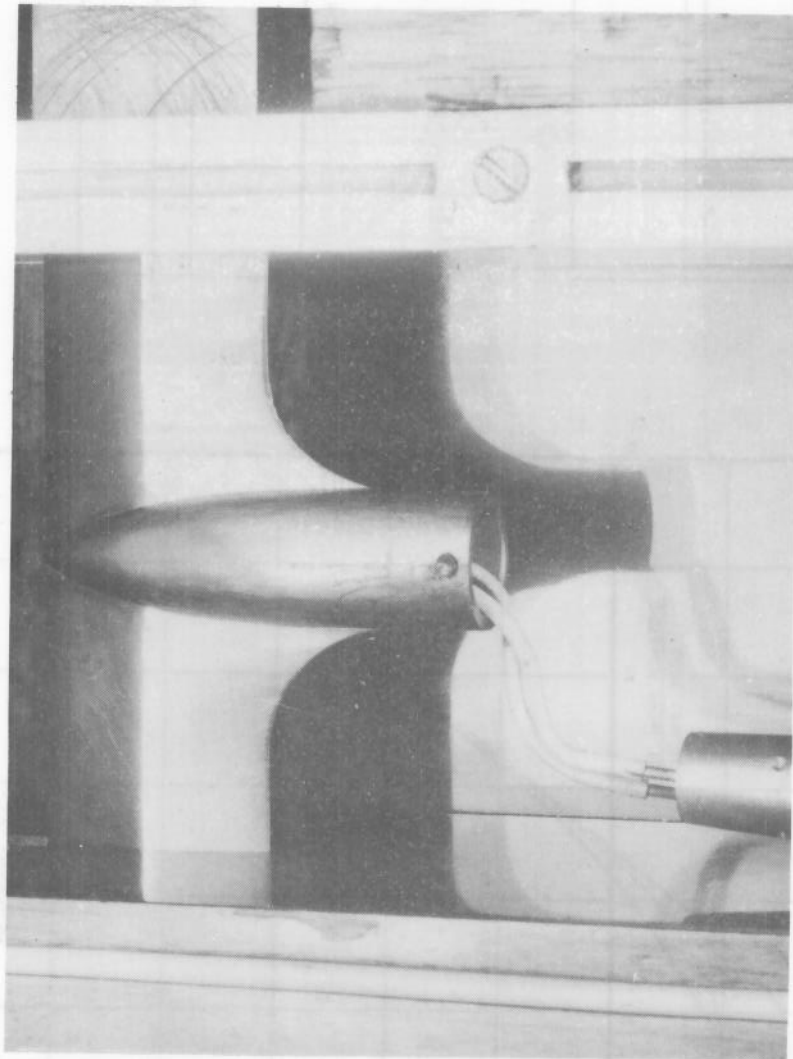


BLOCK DIAGRAM OF THE $2\frac{1}{2} \times 2\frac{1}{2}$
INTERMITTENT SUPERSONIC WIND TUNNEL PLANT.



OGIVES 1, 2, AND 3

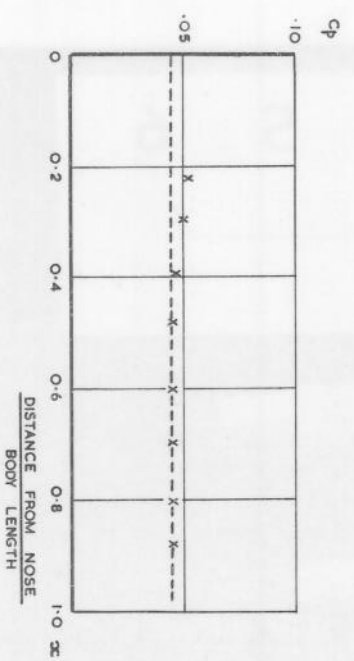
FIG. 4.



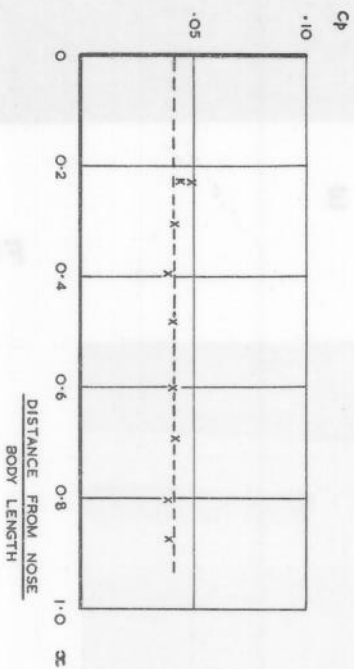
STING SHOWING PRESSURE CONNECTIONS TO THE MODEL

FIGS. 6, 7 & 8.

PRESSURE DISTRIBUTION ON CONE ($\theta_s = 6^\circ 21'$) AT $M = 2.45$



PRESSURE DISTRIBUTION ON CONE ($6^\circ 21'$) AT $M = 3.19$



PRESSURE DISTRIBUTION ON OGIVE I AT $M = 1.8$
(N.P.L. RESULTS REF. 7)

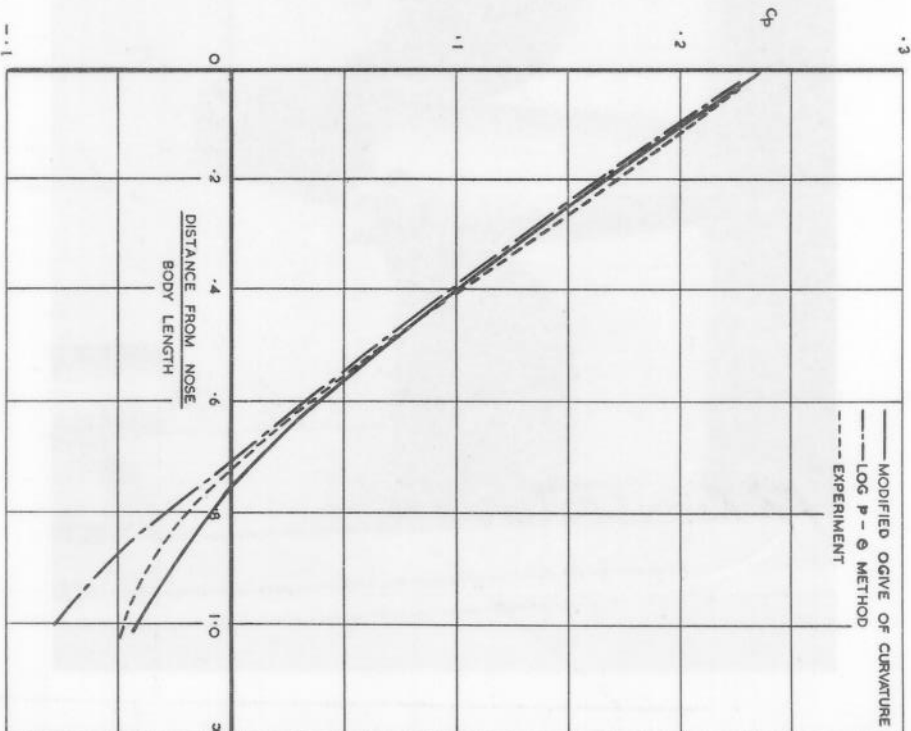


FIG. 6.

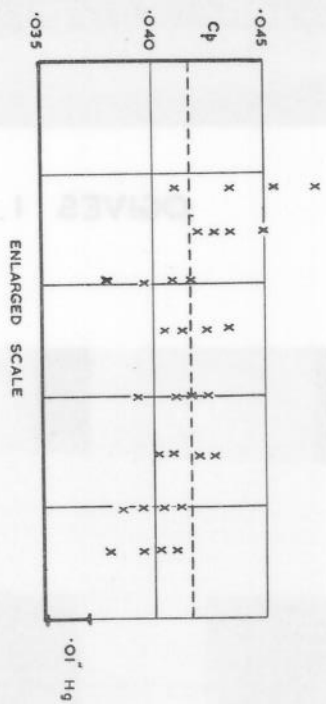
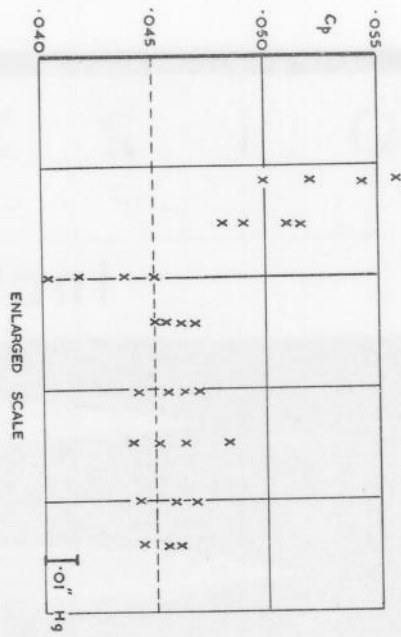
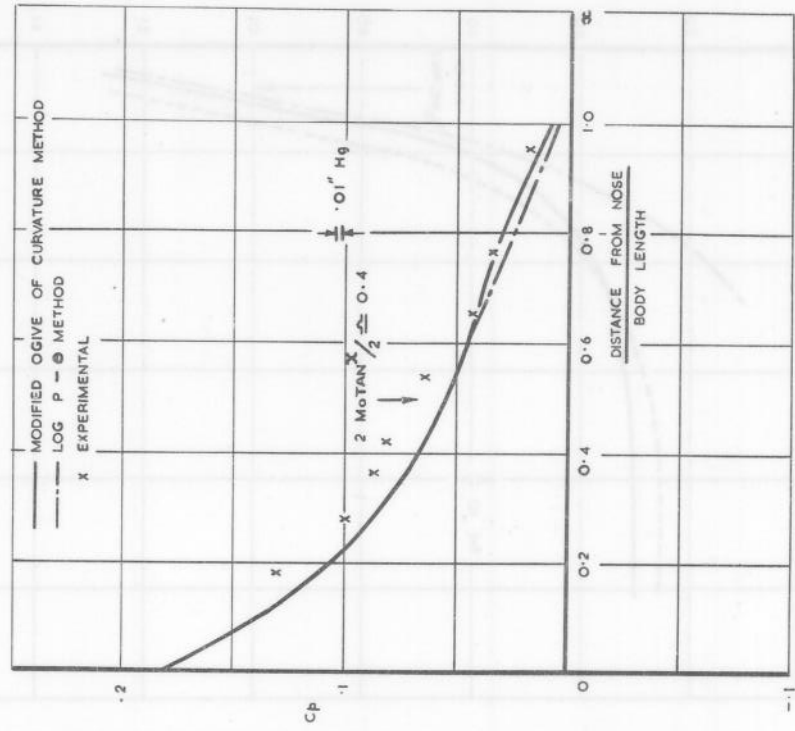


FIG. 7.

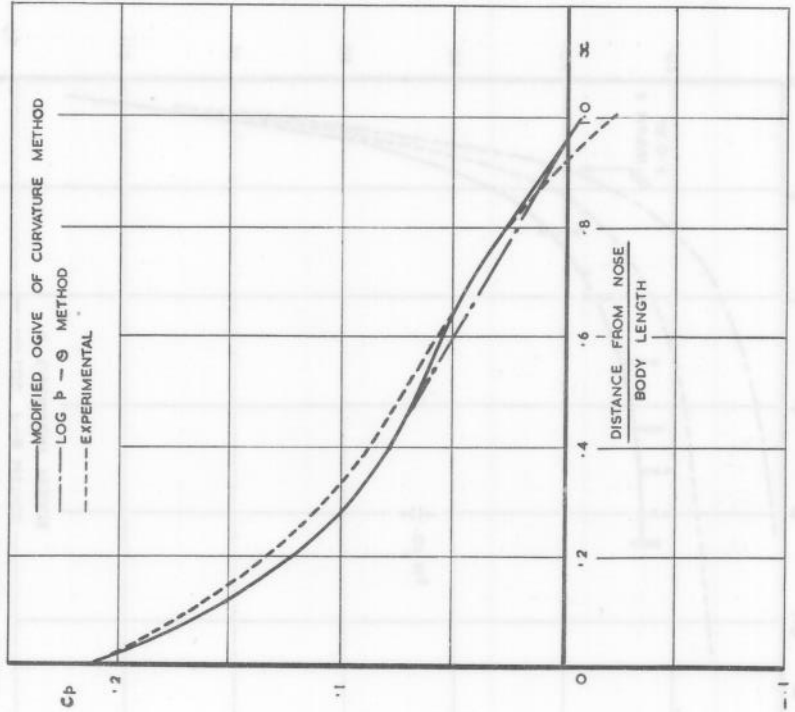
FIG. 8.

FIG. 11



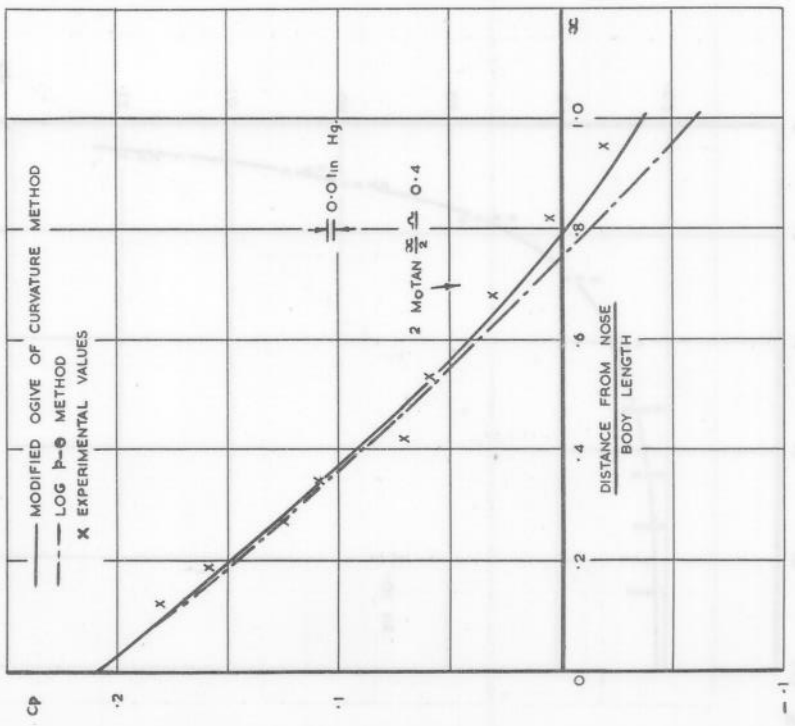
PRESSURE DISTRIBUTION ON OGIVE II AT M=2.45

FIG. 10.



PRESSURE DISTRIBUTION ON OGIVE II AT M = 1.8
 (N.P.L. RESULTS REF. 7)

FIG. 9.



PRESSURE DISTRIBUTION ON OGIVE I AT M = 2.45

FIGS. 12, 13 & 14

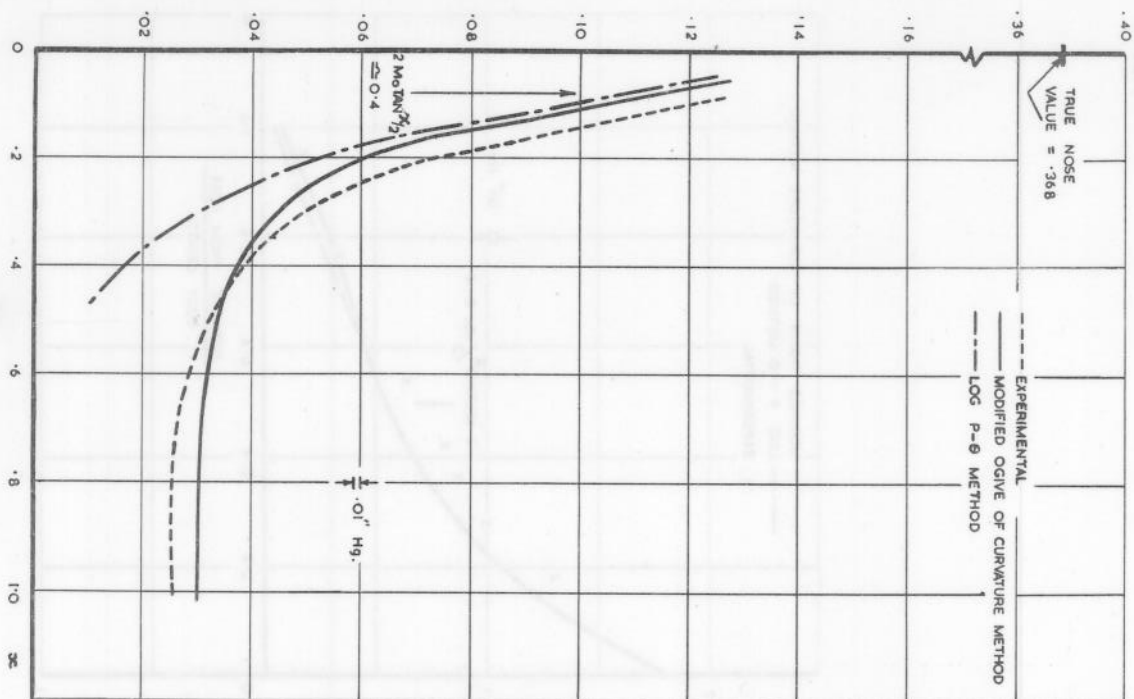


FIG. 12.

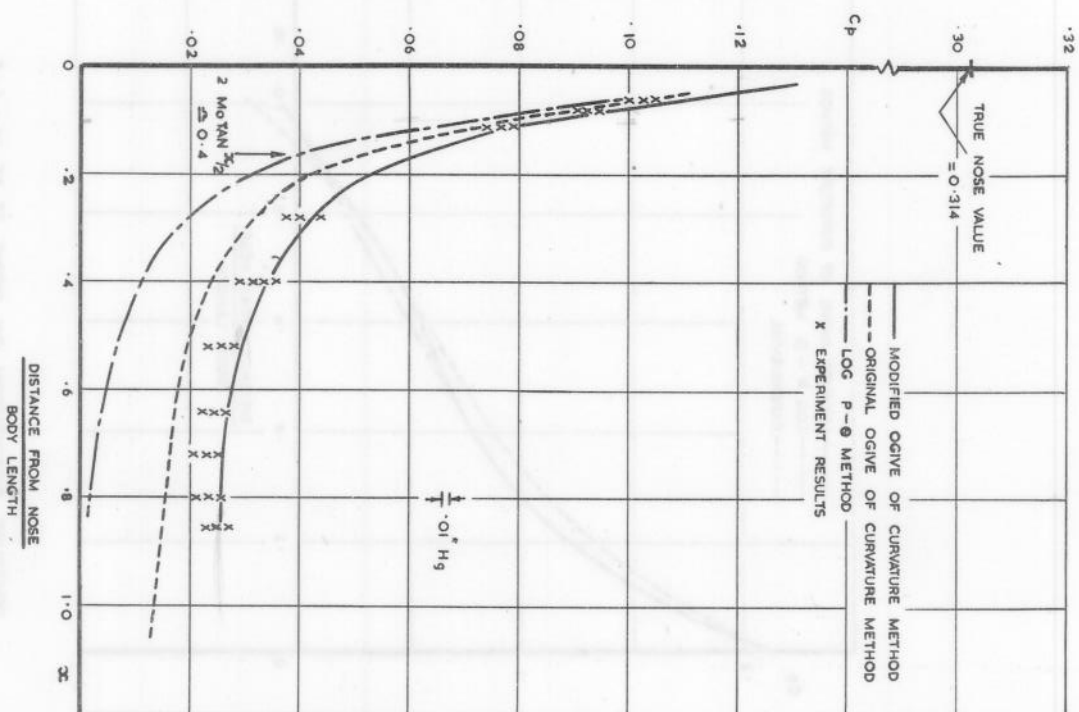


FIG. 13.

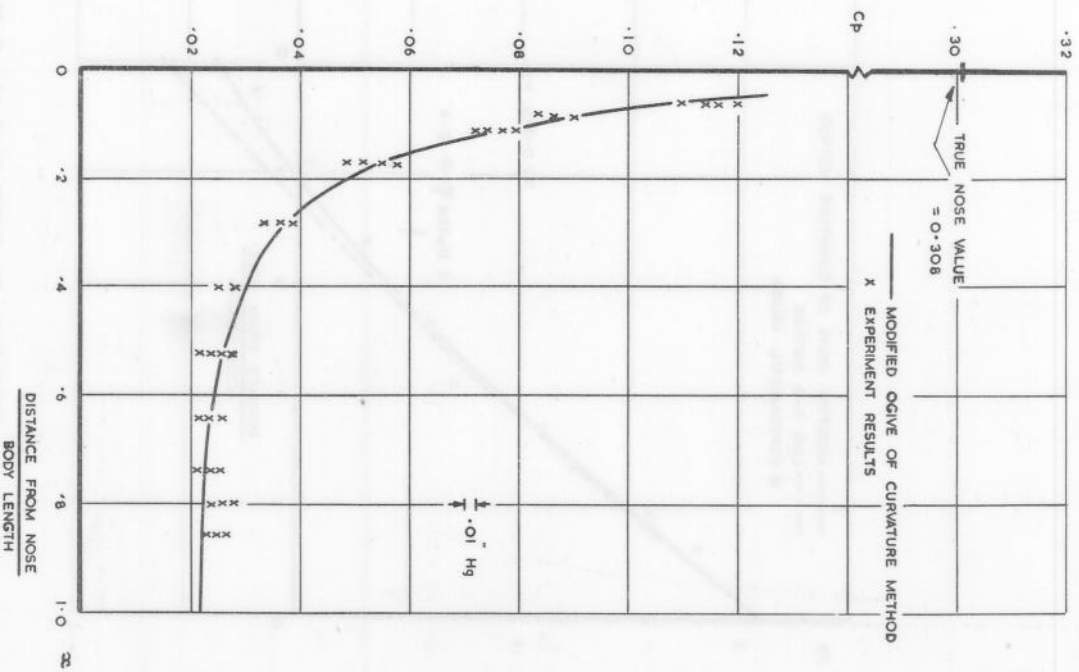


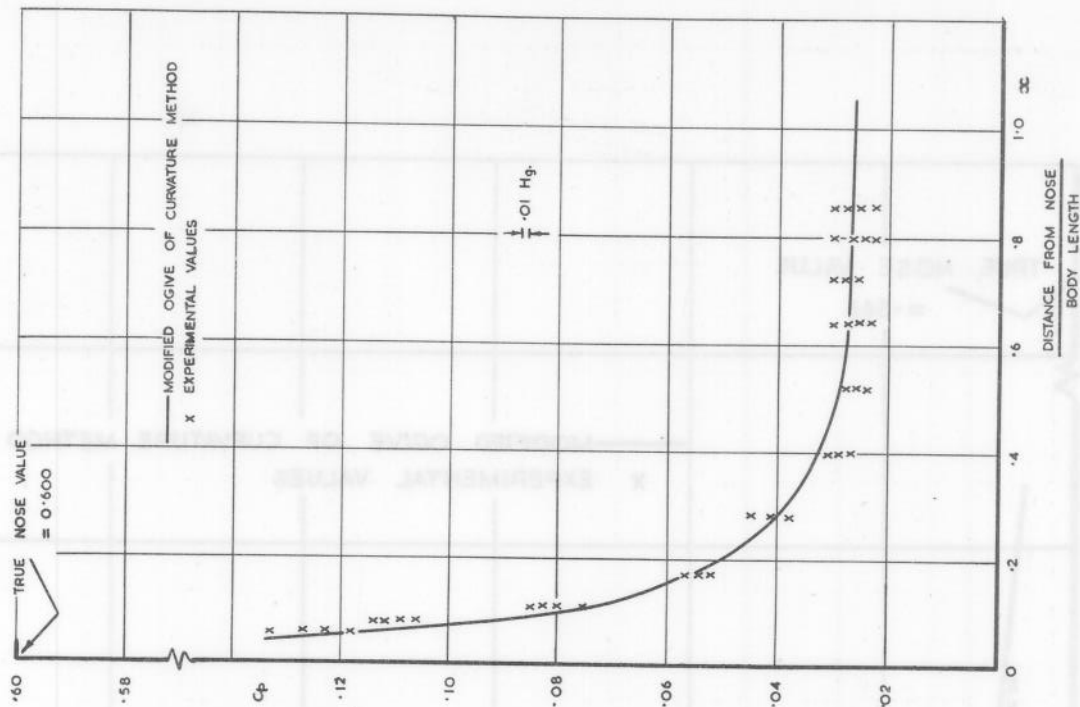
FIG. 14.

PRESSURE DISTRIBUTION ON OGIVE III AT M=1.8
(N.P.L. RESULTS REF. 7)

PRESSURE DISTRIBUTION ON OGIVE III AT M=2.45

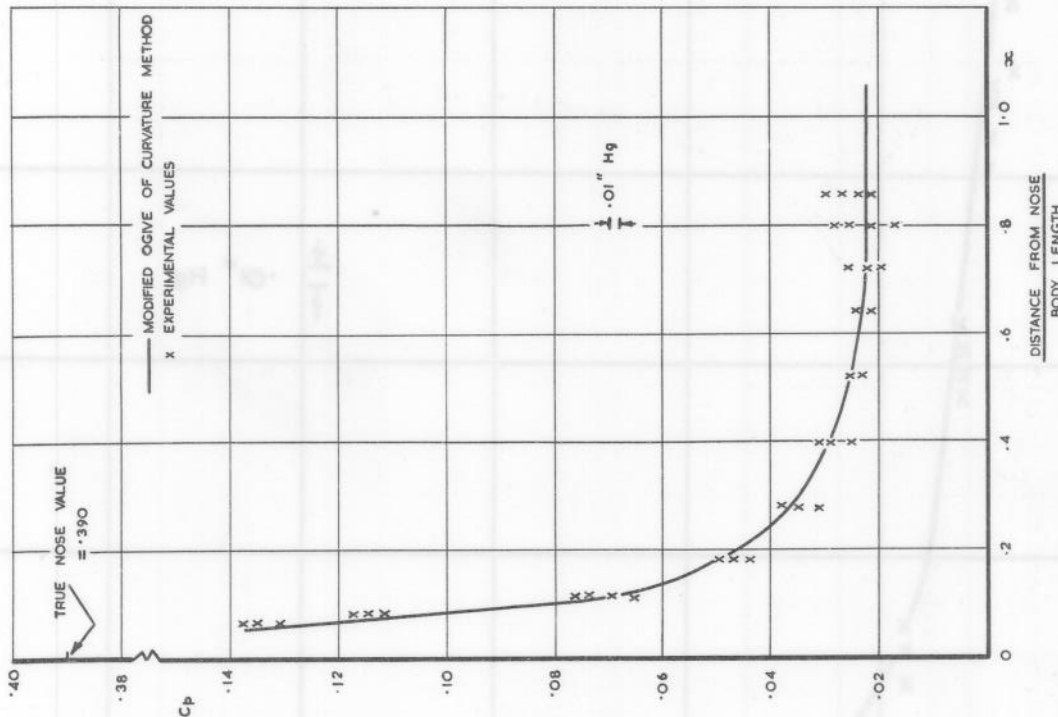
PRESSURE DISTRIBUTION ON OGIVE III AT M=3.19

FIG. 17.



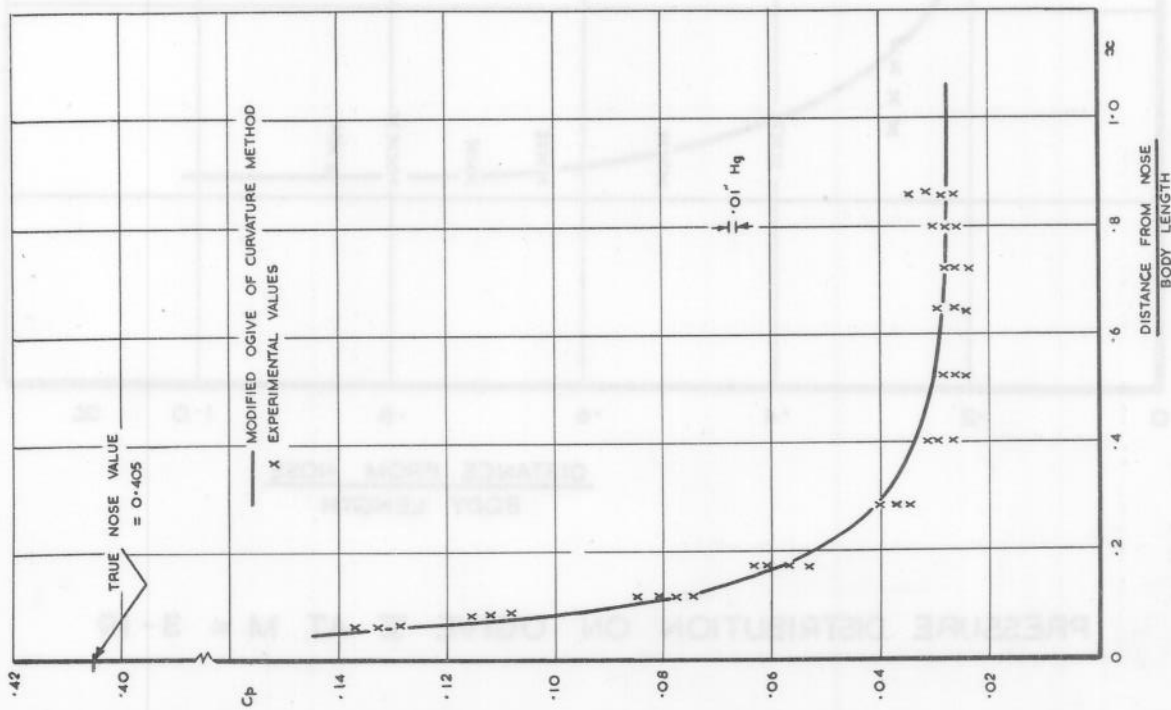
PRESSURE DISTRIBUTION ON OGIVE V AT M = 2.45

FIG. 16.



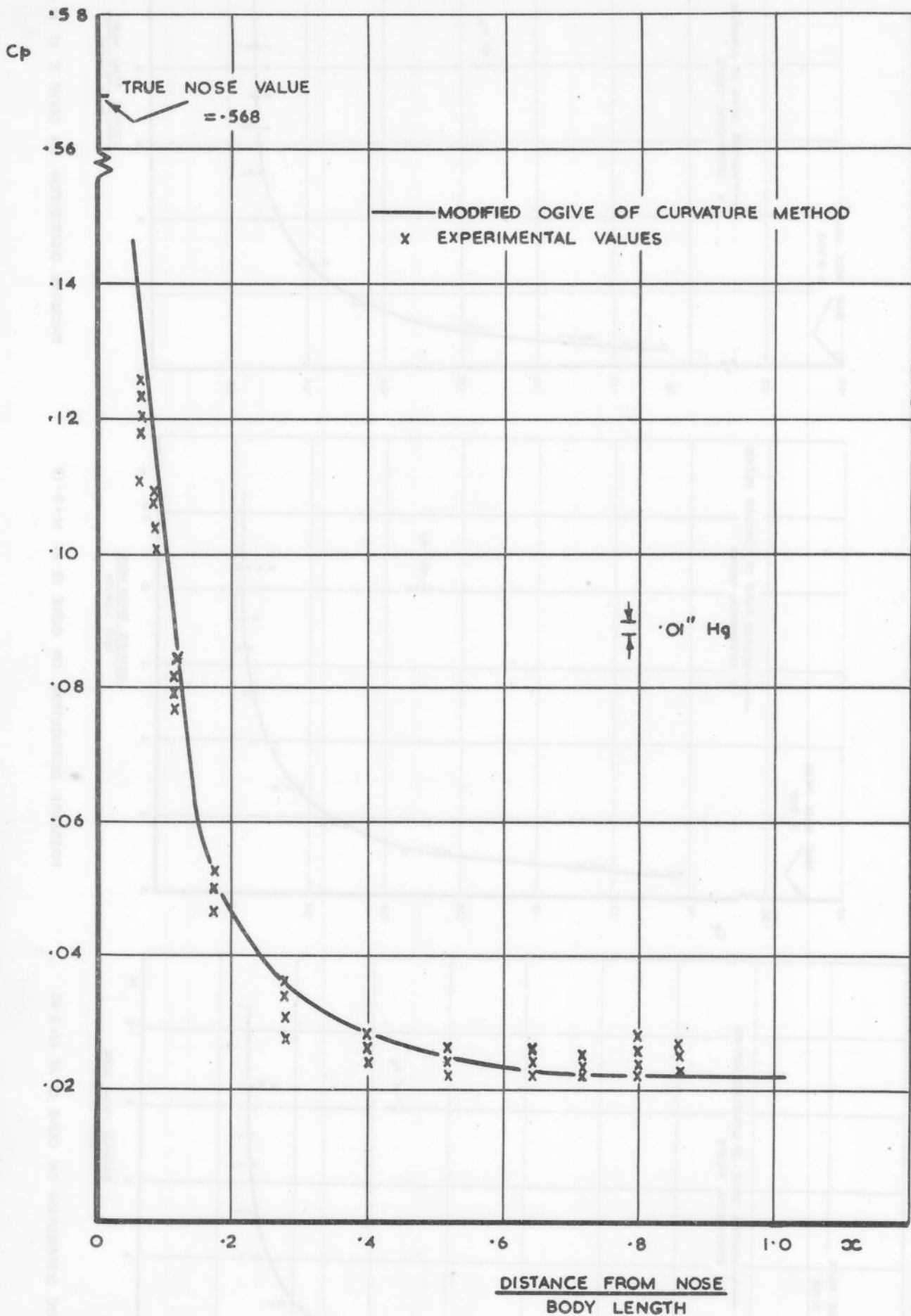
PRESSURE DISTRIBUTION ON OGIVE IV AT M = 3.19

FIG. 15.



PRESSURE DISTRIBUTION ON OGIVE IV AT M = 2.45

FIG. 18.



PRESSURE DISTRIBUTION ON OGIVE V AT M = 3.19